PET/PA Nanocomposite Blends with Improved Gas Barrier Properties: Effect of Processing Conditions

S. Donadi, M. Modesti, A. Lorenzetti, S. Besco

Department of Chemical Process Engineering, Padova University, v. Marzolo 9, Padova 35131, Italy

Received 12 November 2010; accepted 21 February 2011
DOI 10.1002/app.34397
Published online 12 July 2011 in Wiley Online Library (wileyonlinelibrary.com).

ABSTRACT: The aim of this research is to develop nanocomposite polyethylene terephthalate-polyamide blends (PET/MXD6 blends) with low oxygen permeability. Particular attention has been paid to the relation between barrier properties and the processing route adopted and therefore four different strategies were considered. Mechanical characterization shows that clay may effectively act as reinforcing filler in PET/MXD6 blends. Morphological characterization shows the strong effect of the processing strategy on clay dispersion and its distribution between the PET and polyamide phases. Barrier properties of PET/MXD6 nanocomposite blends are enhanced with respect to neat PET polymer as well as PET/MXD6 blends. The significant effect of processing techniques on barrier properties is also revealed. © 2011 Wiley Periodicals, Inc. J Appl Polym Sci 122: 3290–3297, 2011

Key words: blends; processing; barrier; nanocomposites

INTRODUCTION

Several strategies have been proposed to increase the barrier properties of polyethylene terephthalate (PET) to gases (mainly oxygen and carbon dioxide). First, a multi-layer approach, where film of materials with high barrier properties [like ethylene-vinyl alcohol (EVOH) copolymer and aromatic polyamides (PA)] was used in layers with PET. With respect to EVOH, aromatic polyamides retain high barrier properties under conditions of high humidity,[1] making them more suitable for beverage packaging applications.[2] The polyamide of interest is the poly-*m*-xylylene adipamide (MXD6) which has barrier properties an order of magnitude higher than the PET ones.[1,3] The second approach proposed is based on PET blending with high barrier constituent (mainly aromatic polyamides), which shall be dispersed as domains oriented perpendicular to the direction of gas flow thus increasing tortuosity of the diffusion pathway.[4] The main problem related to this approach is the nonperfect compatibility between PET and PA, resulting in yellow color and haziness, observed in oriented blend films and in bottle walls.[5]

Besides multi-layer and blending approaches, a more recent route to increase barrier properties is introducing high shape ratio nanofillers into polymer, most commonly organo-modified layered silicates (OMLS). If platelets are mainly oriented perpendicular to the direction of gas flow, they reduce the gas permeability of the material, due to increased diffusion pathway tortuosity. Moreover, polymer/OMLS nanocomposites exhibit enhanced mechanical strength compared with neat polymers because the dispersed clay layers provide reinforcement in a polymer matrix.[6]

Since it has been recognized that both PET-aromatic polyamides blends and PET-clay nanocomposites have given good results in terms of barrier properties, the aim of this research is to combine these two approaches, thus developing a nanocomposite PET-polyamide blend with low oxygen permeability. Particular attention has been paid to the relationship between barrier properties and the processing routes adopted.

EXPERIMENTAL

Raw materials

Matrix polymer is mainly polyethylene terephthalate (PET 9921, i.e., PET copolymer with intrinsic viscosity of 0.80 dL/g, Eastman Chemical Co. USA) and the disperse polymeric phase is poly(*m*-xylene adipamide) (Nylon MXD6, Mitsubishi Gas Chemical Co. Japan). A commercially available OMLS, i.e., Dellite 72T (D72T), which is a montmorillonite modified with dimethyl dihydrogenated tallow ammonium, provided by Laviosa Chimica Mineraria S.p.A. (Italy) was used. To prevent polymer oxidation during blending, 0.3 wt % of antioxidant (Irganox hp 2225, provided by BASF Germany) was also used.

Correspondence to: M. Modesti (michele.modesti@unipd.it).

Preparation of nanocomposites

The polymeric matrix used in this study is a blend of PET-MXD6, characterized by a weight ratio of 9 : 1, while clay content was fixed at 3.5 wt %. Generally speaking, clay content used in polymer nanocomposites rests between 1 and 5 wt %. According to some of the first lab trials, we choose to fix the clay content at 3.5 wt % because we noticed that 1 wt % was too low to give appreciable results while 5 wt % was too high, resulting in high brittleness.

An unfilled matrix (PET-MXD6 blend) as well as PET-Dellite 72T nanocomposite was also prepared as a reference material.

Nanocomposites were prepared by melt compounding using a corotating, intermeshing twin screw extruder (Collin Teach-line zk25t) with screw diameter (D) of 25 mm and L/D of 30, adopting four different processing routes. A twin screw corotating extruder was chosen because a generally higher intercalation/exfoliation degree is obtained using twin screws as opposed to a single screw extruder, due to an insufficient amount of shear and the shorter residence time in a single screw extruder.[7] Moreover, reprocessing (as in our case) with a single screw extruder, can result in re-agglomeration of the silicate layers that instead should be avoided.[8]

Before processing, to avoid polymer hydrolysis, PET, MXD6 and clay were dried at 80°C for 48 h *in vacuo*.[1,9]

Using melt blending techniques to prepare nanocomposite blends, two general approaches are feasible: a one-step process, in which the polymers and clay are dry-premixed or fed separately to the extruder in the correct proportions, and a two-step process, where the final nanocomposite blend is obtained by the dilution of a concentrate masterbatch. Considering that the clay has higher affinity with aromatic polyamides than polyethyleneterephthalate,[10] four different processing strategies have been studied with the aim to create a structure as homogeneous as possible, in which domains of nylon and nanofillers in PET were equally distributed, to maximize the barrier effect.

The four processing strategies used to prepare nanocomposites are the following.

1. In the first step MXD6 and clay were mixed by melt blending. During a second extrusion step, that material was diluted with PET to get the desired composition (Method 1).
2. in the first step a PET–clay nanocomposite was extruded and then MXD6 was added in a second step (Method 2).
3. Nanocomposites were obtained by a one-step method, i.e., they were prepared by melt mixing of PET/MXD6/clay in the right proportions with a single extrusion step (Method 3).
4. Matrix blend was prepared by melt compounding PET and MXD6; after that, clay was added in a second extrusion step (Method 4).

During the first extrusion step of Method 1, 2, and 4, the temperature profile of the extruder chamber, from hopper to die, was 210-250-250-250-245°C and a screw speed of 35 rpm was used. During the second extrusion steps of those methods and also for the single step procedure (Method 3), a profile of 210-260-260-260-255°C and screw speed of 100 rpm was imposed. Extruder temperatures were set low enough to limit acetaldehyde generation and allow high shear stress generation; temperatures may not be too low to prevent excessive melt viscosity. Degassing at −0.4 bar in the middle of chamber was used to remove vapor and other gases.

After every extrusion, all materials were dried at 160°C for 4 h under 4 kg/h air flow before further processing or characterization.

Henceforth, samples will be identified by M1, M2, M3, and M4 according to the method number (from 1 to 4) used for their preparation.

NANOCOMPOSITES CHARACTERIZATION

Mechanical tests

The specimens for mechanical characterization were injection molded. Tensile properties were measured using a dynamometer (Galdabini, mod. Sun 2500); the tests were carried out according to ASTM D-638. The flexural modulus was determined using the same dynamometer with a three-point loading test, according to ASTM D-790. For each sample, the values reported are the mean of five measurements; also the standard deviations are provided in the graphs.

Differential scanning calorimetry

The analysis of the crystallinity was carried out by means of differential scanning calorimetry (DSC) using TA Instruments DSC Q200. The specimens were placed in sealed aluminum cups and then cyclically heated and cooled from 40 to 280°C, using a heating rate of 10°C/min and a cooling rate of 5°C/min. The heat of crystallization of the samples was measured after melting the specimen to delete the thermal and mechanical history.

Dynamic mechanical analysis (DMA)

A dynamic mechanical analyzer (DMA, TA Instruments model 2980) was used to assess the dynamic

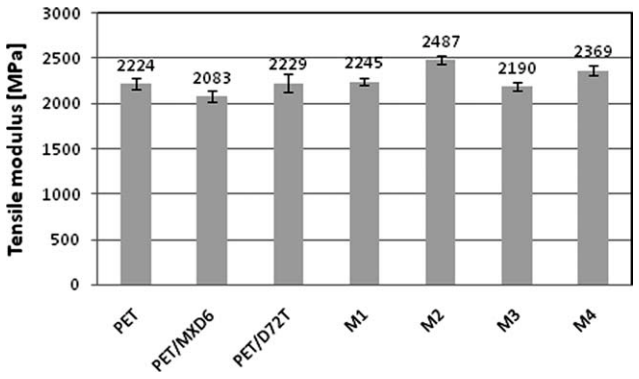

Figure 1 Tensile modulus of all materials prepared.

mechanical performance of the composites prepared: the analyses were carried out by oscillating the samples in the single-cantilever mode (flexural method) at a frequency of 1 Hz, amplitude of 15 μm, and heating rate of 5°C/min between −50 and 150°C. The specimens were obtained by means of injection molding in a rectangular geometry.

Deflection temperature under load

Analysis of the deflection temperature under load (DTUL) is standardized by ASTM D-648 and represents a method of assessment of the softening temperature of a material. Samples with a rectangular section were analyzed in the three point bending mode in the DMA analyzer. The samples were subjected to a constant bending load of 0.455 MPa and simultaneously their temperature was increased by 2°C/min. The DTUL is the temperature at which a deflection of 0.25 mm is observed. The analyses were performed with the DMA (TA instruments) 2980.

X-ray diffraction

The degree of intercalation and exfoliation of the clay were monitored by X-ray diffraction (Philips model X'PERT PRO). The XRD analyses were carried out in reflectance mode with Cu anode material ($K_{\alpha 1} = 1.54056$ nm, $K_{\alpha 2} = 1.54439$ nm). The diffractograms were scanned in a 2θ range from 1.50 to 12.50° at scan rate of 0.02°/s, 40V generator voltage.

Interplane distances d are calculated using Bragg's Law:

$$\lambda = 2d\text{sen}\vartheta$$

where the wavelength λ is 1,541837 Å.

Transmission electron microscopy (TEM)

The level of dispersion was investigated also by high magnification transmission electron microscopy (TEM, Philips model EM 208) using an acceleration voltage of 100 kV. Samples for TEM analyses were cut from ultra-thin specimens using a Leica Ultracut UCT ultramicrotome.

Oxygen gas permeability test

The barrier effect, due to layered silicates, was investigated by a permeability tester (Extrasolution, MultiPerm), testing 50 cm^2 quenched thin films under 11.2 mL/min oxygen gas flow, at 22°C and 50% relative humidity according to ASTM F 2622. The values reported are the mean of three measurements and standard deviations are provided in the graphs.

RESULTS AND DISCUSSION

Mechanical tests

Figure 1 shows tensile modulus for all the samples prepared. MXD6 is characterized by a higher tensile modulus (about 4.7 GPa) than neat PET, thus a small increase (considering the low amount of MXD6 used, about 10 wt %) of such property might be expected for PET/MXD6 blends. Otherwise, when PET and MXD6 are blended, a little decrease of tensile modulus with respect to neat PET is observed, owing probably to the partial immiscibility between two polymers. PET/D72T nanocomposites show no increase of tensile modulus with respect to pure PET due probably to the poor clay dispersion obtained by single-step processing. Contrarily, PET/MXD6/D72T nanocomposites show an increase with respect to the corresponding unfilled matrix for every processing method used. Tensile modulus of PET/MXD6 nanocomposites blends are similar, or in some cases even better, than that of neat PET.

Better results were obtained using Method 2 (M2 sample) and 4 (M4 sample). This means that, using suitable processing conditions, the clay may effectively act as reinforcing filler in such materials, thus limiting negative effects on mechanical properties of PET/MXD6 blends. Figure 2 shows maximum tensile

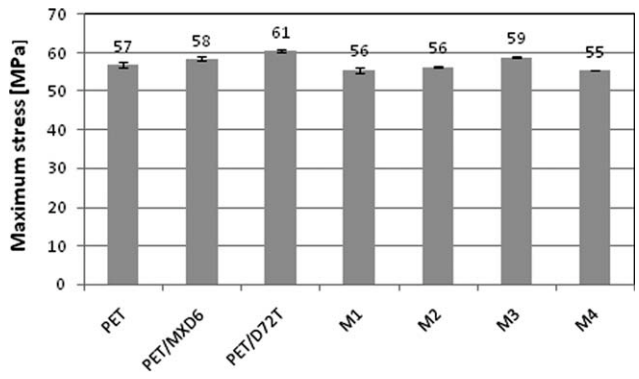

Figure 2 Average values of maximum tensile stress of all materials.

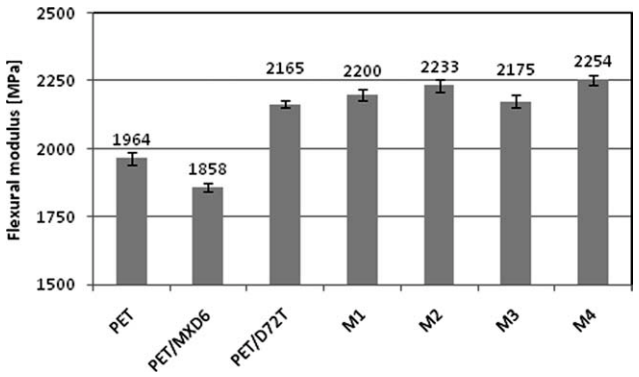

Figure 3 Flexural modulus of all materials.

stresses of all materials. No significant differences can be observed for all the materials tested. Figure 3 shows flexural modulus of all materials with trends similar to that of tensile modulus. The blending of MXD6 with PET leads to a decrease of flexural modulus, but this drawback may be overcome by adding clay. No strong effects due to processing methods used can be inferred from the data obtained, although slightly better results are obtained for Method 2 and 4.

As morphological results (XRD and TEM analyses) will show different processing methods lead to different clay dispersion degrees, which are responsible for the variations of mechanical properties observed. It will be shown that the PET/D72T sample is characterized by the poorest clay dispersion and thus no enhancement of mechanical properties, with respect to the neat PET matrix, can be expected. The other nanocomposites show a better clay dispersion and that is responsible for the slight improvement in mechanical properties of these nanocomposites, with respect to the unfilled PET/MXD6 sample. Moreover, it will also be shown by TEM analyses that processing methods affect the size of MXD6 domains, which influence the mechanical properties of the blends, since it is known that the smaller the domains the better the mechanical properties.[11]

Differential scanning calorimetry

DSC thermograms of neat PET polymers and the PET/MXD6 blend matrix are reported in Figure 4(a,b). It is known[12] that PET and MXD6 are immiscible polymers, thus two different glass transition temperatures (T_g) are expected. However, as these temperatures are very close to each other, they are not distinguishable, so the matrix shows only one T_g as already reported in other works.[13] A nucleating effect of MXD6 can be observed, since crystallization of PET takes place at higher temperatures (i.e., a lower subcooling degree is required) and the crystallization peak is sharper. No particular effect of MXD6 was shown on the melting behavior of PET

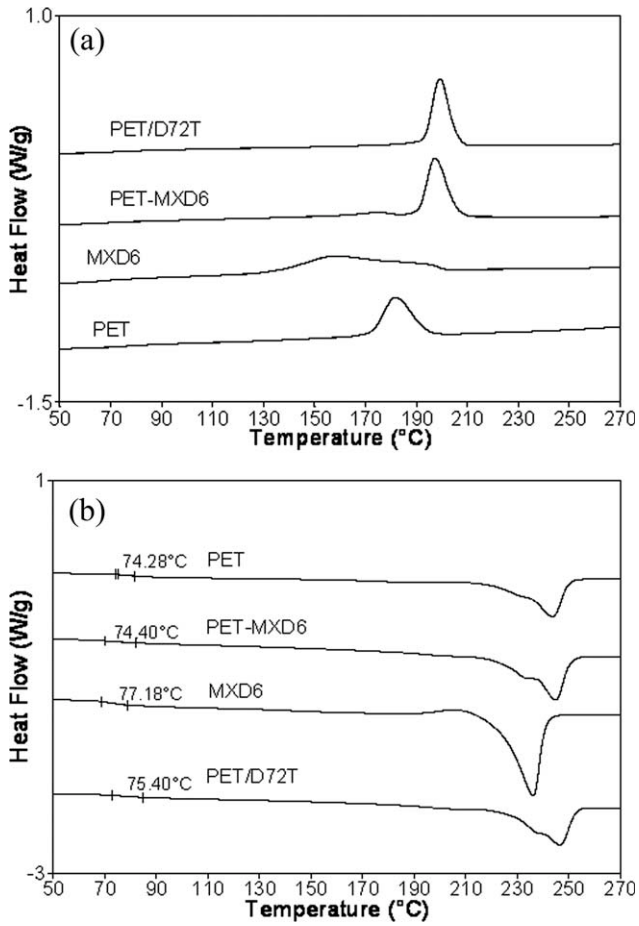

Figure 4 DSC thermograms of PET, MXD6 and PET/MXD6 blend: (a) cooling rate 5°C/min, (b) heating rate 10°C/min.

polymer. The same effect was seen when D72T clay was blended with PET: the clay acts as nucleating agent, thus favoring crystallization, while no significant difference was observed for the melting behavior of neat PET or PET nanocomposite [Fig. 4(b)].

More details on DSC results for PET, MXD6, PET/MXD6 blend, and nanocomposites as well as nanocomposite blends are reported in Table I.

TABLE I
DSC Results of PET, MXD6, PET/MXD6 Blend, PET/D72T and PET/MXD6/D72T Nanocomposites (Cooling Rate 5°C/min, Heating Rate 10°C/min)

Sample	T_g (°C)	T_c (°C)	ΔH_c (J/g)	T_m (°C)
PET	74	181	42	244
MXD6	77	158	53	237
PET/MXD6	74	197	49	245
PET/D72T	75	199	46	247
M1	71	196	46	246
M2	71	197	45	245
M3	73	195	42	246
M4	71	196	42	246

T_g = glass transition temperature; T_c = crystallization temperature; ΔH_c = total heat of crystallization; T_m = melting temperature.

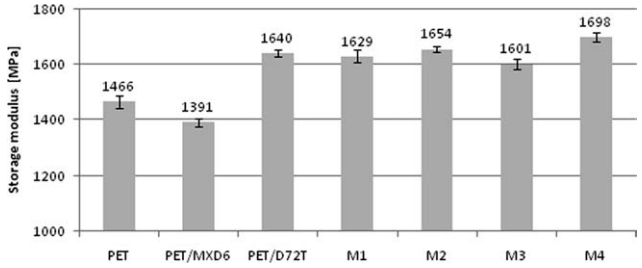

Figure 5 Storage modulus at room temperature measured by DMA of all materials.

In accord with the results reported, favorable effects on PET crystallization were seen also for PET nanocomposites blends, since crystallization temperature (T_c) increases in the presence of clay and/or MXD6. No important variations of glass and melting temperature were observed for PET nanocomposites and for PET/MXD6 nanocomposite, irrespective of the processing method used.

Dynamic mechanical analysis (DMA)

Analyzing Figure 5, it is immediately clear that the trend of storage modulus at room temperature in single-cantilever mode is very similar to that already reported for static flexural modulus. It is evident that the presence of clay leads to an increase of storage modulus for both neat PET and PET/MXD6 blends; better results were obtained using processing Method 4.

Evaluations of glass transition temperature measured by peak of loss modulus in DMA analysis are in agreement with the DSC results and no significant variations were observed for both PET and PET/MXD6 blend filled materials. Results of peak of loss modulus for all the samples prepared are reported in Figure 6.

Deflection temperature under load

The results of DTUL measurements are reported in Figure 7. It can be clearly seen that no significant differences arise due to the presence of clay.

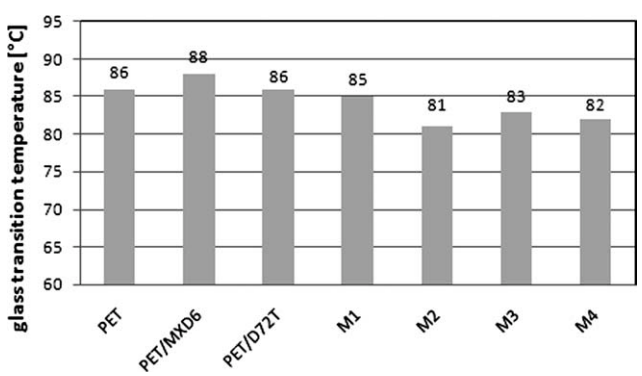

Figure 6 Glass transition temperature, evaluated by loss modulus peak, for all samples prepared.

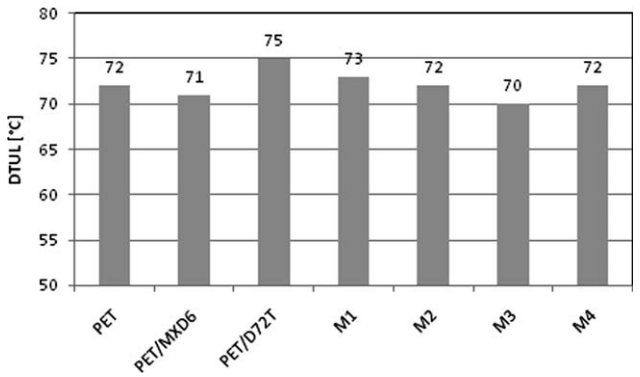

Figure 7 Values of DTUL of all samples prepared.

X-ray diffraction

XRD analyses were carried out on neat polymers, filler, and nanocomposites to study the morphology and quantify clay intercalation. Figure 8 shows XRD spectra of neat PET and MXD6 polymers, PET/MXD6 blend, pure clay and nanocomposite blends. It can be observed that the main diffraction peak of clay ($2\Theta = 3.38°$) shifts to lower angles for both PET nanocomposite and nanocomposite blends, thus showing clay intercalation; differences between processing routes are negligible. XRD spectra also show small humps between 5 and 6°; these may be due to second order basal reflection which is consistent with a well ordered system of stacked clay layers[13] and/or to tactoids, i.e., not intercalated clays, whose presence is confirmed by TEM analysis.

2Θ angles as well as interplanar distance of the samples prepared, calculated using Bragg's law, are reported in Table II. The best results were obtained for Method 1 (M1) sample which has a slightly higher interplanar distance. Method 1 promotes probably a selective dispersion in MXD6 phase (since the clay was first dispersed in MXD6, and then PET was added after that) which shows a higher affinity to clay than PET, leading to an higher level of intercalation.

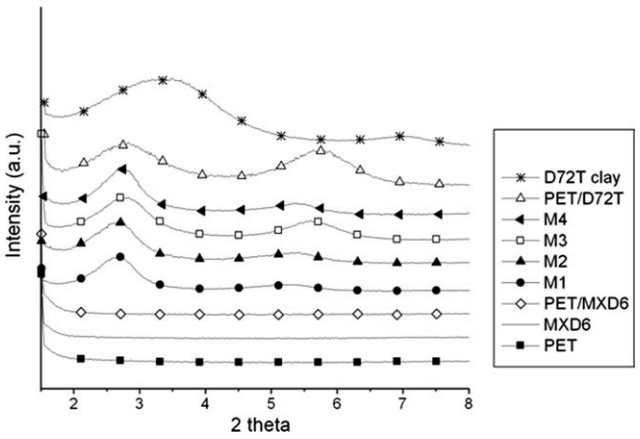

Figure 8 XRD spectra of PET, MXD6, PET/MXD6 blend, nanocomposite PET, nanocomposite blends and D72T clay.

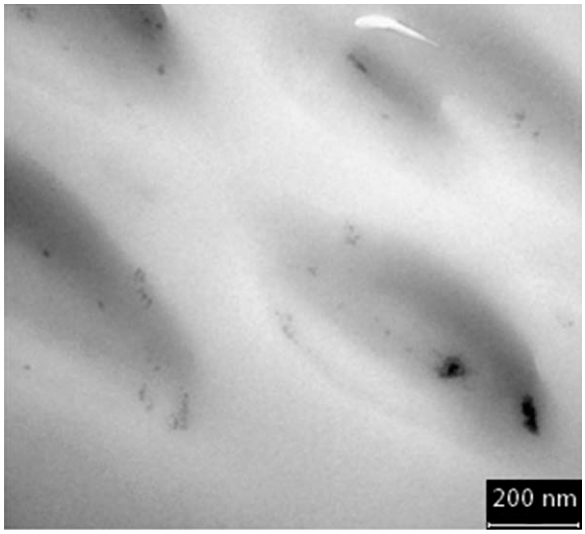

Figure 9 TEM image of PET/MXD6.

Transmission electron microscopy (TEM)

TEM analyses can be used to evaluate nanocomposites blends structure, showing phase separation of matrix, clay dispersion, and clusters presence. TEM image of PET/MXD6 matrix (Fig. 9) shows isolated domains of MXD6 phase dispersed into PET phase.

Since both the dimensions and dispersion of these domains as well as clay layers have a role to improve barrier properties,[4] both those features have been analyzed by TEM for all nanocomposite blends prepared.

Generally, a preferential dispersion of clay into MXD6 domains has been observed, in particular for M1 materials. Figure 10 shows TEM image for PET nanocomposites blend obtained by Method 1, i.e., addition of PET to already mixed MXD6/clay material. A preferential clay presence can be observed, inside MXD6 domains instead of PET continuous phase. The clay seems to be mainly intercalated although some small tactoids can be seen at lower magnification.

A comparison between processing routes can be drawn analyzing Figures 10 and 11, where TEM images of M2, M3, and M4 samples are reported. Irrespective of the processing method used, it can be noted that MXD6 domains in nanocomposites have smaller dimensions than those of unfilled PET/MXD6 blend. Moreover, as it was expected, the dispersion of clay is generally better for two-step procedures (particularly the M2 method) with respect to the single-step procedure (M3 method). In terms of clay distribution, the best results have been obtained using processing Method 2, i.e., first dispersing clay in PET polymer and, after that, blending PET filled polymer with MXD6. This may be due to the higher affinity of clay toward MXD6: indeed, when clay is dispersed first in MXD6 (Method 1), the diffusion of clay towards PET phase during the second step of melt blending is hindered by the low affinity of clay towards PET itself. Contrarily, when clay is dispersed first in PET (Method 2), the subsequent diffusion of clay toward MXD6 phase during the second step of melt blending is favored by chemical affinity: the thermodynamic driving force was indeed strong enough to overcome the high viscosity of the PET phase, thus recapturing part of the clay in MXD6 phase on melt-blending. Similar results were already reported for nanocomposite blends comprising PET or polyamides.[15,16] In Method 4, clay is added

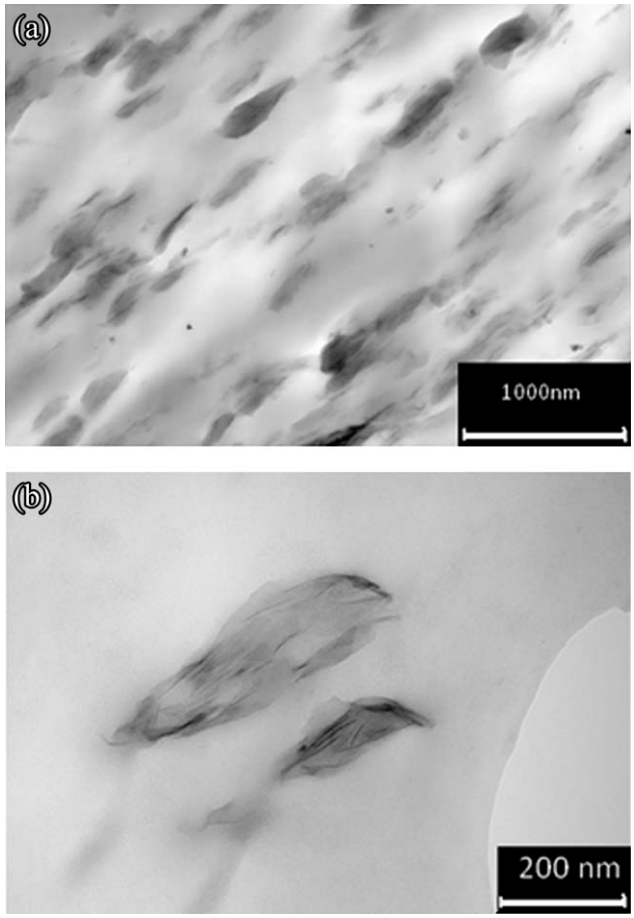

Figure 10 TEM images of M1 nanocomposites at lower (a) and higher (b) magnification.

TABLE II
Interplanar Distances of Nanocomposites Calculate Using Brag Law from XRD Measurements

Sample	Angle Θ [rad]	Interplane distance *d* [Å]
D72T clay	0.0295	26.11
PET/D72T	0.0250	30.89
M1	0.0229	33.63
M2	0.0234	32.91
M3	0.0245	31.45
M4	0.0239	32.22

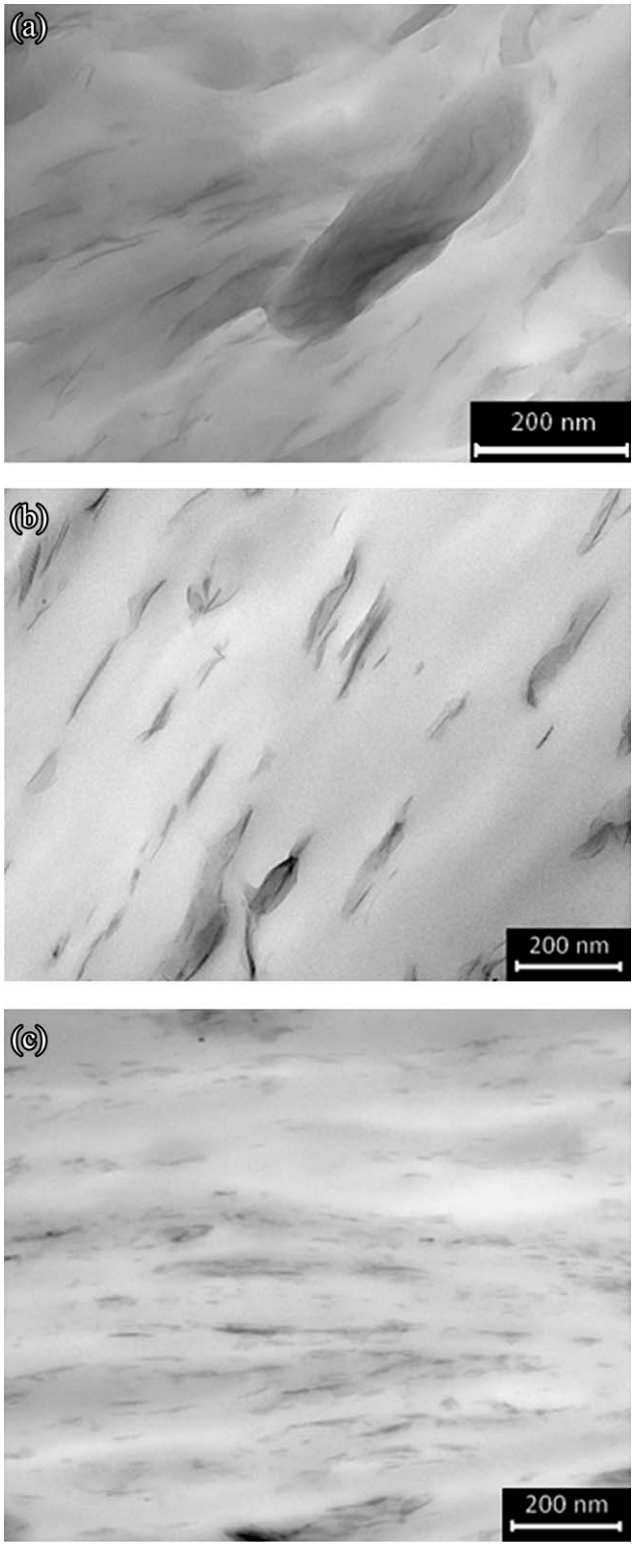

Figure 11 TEM images of M2 (a), M3 (b), and M4 (c) nanocomposites.

simultaneously to both PET and MXD6 phases during the second step of melt blending (it is not predispersed in one single phase), thus a higher amount of clay diffuses towards the PET phase with respect to Method 1.

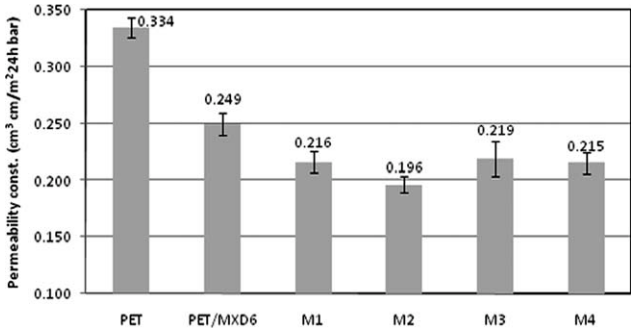

Figure 12 Oxygen permeability constant for all samples.

Summarizing, it seems that an important feature in processing of polymer nanocomposites blends is first dispersing clay in the low-affinity phase (i.e., the PET phase), since, in the second step, due to better thermodynamic interactions, clay tends to diffuse easily toward the higher affinity phase (i.e., MXD6).

Oxygen permeability test

The effect on barrier properties arising from PET/MXD6 blending and PET/MXD6 nanocomposite

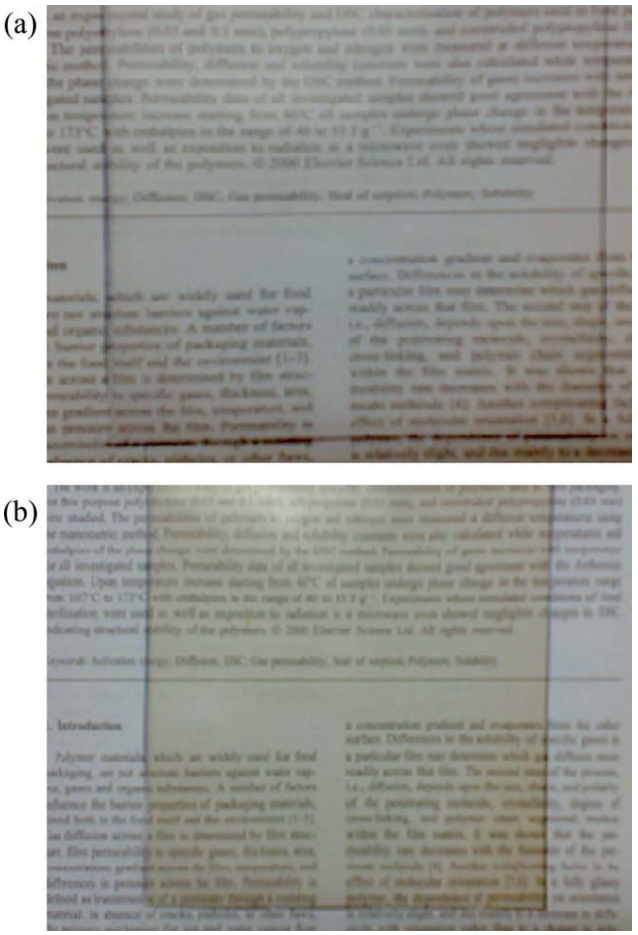

Figure 13 Sheets of PET/MXD6 (a) and M2 (b) samples [Color figure can be viewed in the online issue, which is available at wileyonlinelibrary.com.].

development is evaluated by O_2 permeability tests. Comparison of the effect of processing methods have been carried out, as reported in Figure 12.

The oxygen permeability of PET film obtained here is slightly lower than that of literature (e.g., 0.363[13] or 0.383[17] cm^3 cm m^{-2} atm^{-1} day^{-1}). The data obtained confirms the already well known improvement given by blending of MXD6 to PET, owing to the high barrier properties of MXD6 itself. The result obtained for PET/MXD6 blend is similar or better to those reported in the literature for unoriented film such as, for example, 0.303[13] or 0.295[17] cm^3 cm m^{-2} atm^{-1} day^{-1} for 90/10 PET/MXD6 blend.

Addition of clay to PET/MXD6 blend results in a further reduction of the oxygen permeability constant by about 10–20% (Fig. 12). Even if there are only slight variations depending on the processing method used, especially for the M1, M3, and M4 samples, some differences may be observed. Generally speaking, these variations are related to the different degrees of intercalation and distribution of the clay in the polymeric matrix. When the clay is more homogeneously distributed between the two polymeric phases and more intercalated, the oxygen permeability is lower. Indeed, the permeability constant is the lowest for M2, owing probably to better dispersion of clay in the PET phase with respect to other methods, thanks to the first step of mixing of PET and filler. The single step method (Method 3) gives a slightly higher permeability constant, probably owing to the predominant dispersion of clay in the MXD6 phase and the lower intercalation degree achieved. Method 4, due to the addition of the clay to an already formed PET-MXD6 blend, allows the dispersion of clay not only in MXD6 domains but also in PET phase, resulting in slightly better barrier properties than M3 sample. The dispersion of PET in an already formed MXD6-clay blend (Method 1) seems to give slightly worse results than M4, probably owing to the very low amount of clay in the PET phase (as shown by TEM results); however, differences between M1 and M4 are almost negligible.

Finally, regarding optical transparency, which is a very important property for barrier application: all filled samples show low yellowness, due to clay impurities, although they are still transparent, as can be confirmed analyzing Figure 13 showing PET/MXD6 [Fig. 13(a)] and the M2 sample [Fig. 13(b)].

CONCLUSIONS

PET/MXD6 nanocomposite blends with improved oxygen barrier properties have been successfully developed. It was shown that the processing strategy deeply influences morphological and barrier properties.

Mechanical characterization showed that, when using a suitable processing method, the clay may effectively act as reinforcing filler in PET/MXD6 blends, thus limiting negative effects on the mechanical properties of such blends.

Morphological characterization showed that the processing method used influenced significantly the clay dispersion in PET or MXD6 domains. A better clay dispersion was obtained by first dispersing clay in the low-affinity phase (i.e., the PET phase), and then adding the high-affinity phase (i.e., MXD6) since, clay tends to diffuse easily toward the higher affinity phase, in the second step.

The barrier properties data obtained confirm the already well known improvement given by blending of MXD6 to PET, owing to the high barrier properties of MXD6 itself. Further introduction of 3.5 wt % of clay results in a further reduction of the oxygen permeability constant by about 10–20%. Since the processing method affects clay distribution between PET and MXD6 phases, also the barrier properties show a dependency on the processing techniques analyzed. Better barrier properties were obtained using a two step procedure, when clay was first dispersed in the low-affinity PET phase and, then the higher affinity MXD6 phase was blended.

References

1. Hu, Y. S.; Mehta, S.; Hiltner, A.; Baer, E. J Polym Sci Part B: Polym Phys 2005, 43, 1365.
2. Turner, S. R.; Connell, G. W.; Stafford, S. L.; Hewa, J. D. WO0109245 2001.
3. Rajagopalan, P.; Kim, J. S.; Brack, H. P; Lu, X.; Eisenberg, A.; Weiss, R. A.; Risen, W. M. J Polym Sci Part B: Polym Phys 1995, 33, 495.
4. Subramanian, P. M.; Mehra, V. Polym Eng Sci 1987, 27, 663.
5. Maruhashi, Y.; Iida, S. Polym Eng Sci 1987 2001, 41.
6. Hasegawa, N.; Okamoto, H.; Kato, M.; Usuki, A.; Sato, N. Polymer 2003, 44, 2933.
7. Pavlidou, S.; Papaspyrides, C. D. Prog Polym Sci 2008, 33, 1119.
8. Russo, G. M; Nicolais, V.; Maio, L. D.; Montesano, S.; Incarnato, L. Polym Degrad Stab 1925 2007, 92.
9. Frounchi, M.; Dourbash, A. Macromol Mater Eng 2009, 294, 68.
10. Hussain, F.; Hojjati, M.; Okamoto, M.; Gorga, R. E. J Comp Mater 2006, 40, 1511.
11. Robeson, L. M. Polymer Blends: A Comprehensive Review; Hanser Gardner Publications: Munich, 2007.
12. Özen, I.; Bozoklu, G.; Dalgçdir, C.; Yücel, O.; Ünsal, E.; Çakmak, M.; Menceloglu, Y. F. Eur Polym Mater 2010, 46, 226.
13. Prattipati, V.; Hu, Y. S.; Bandi, S.; Schiraldi, D. A.; Hiltner, A.; Baer, E.; Mehta, S. J Appl Polym Sci 2005, 97, 1361.
14. Modesti, M.; Besco, S.; Lorenzetti, A.; Causin, V.; Marega, C.; Gilman, J. W.; Fox, D. M.; Trulove, P. C.; De Long, H. C.; Zammarano, M. Polym Degrad Stab 2007, 92, 2206.
15. Besco, S.; Lorenzetti, A.; Roso, M.; Modesti, M.; Polym Adv Technol 2011, 22 , DOI: 10.1002/pat.1641.
16. Manias, E.; Heidecker, M. J.; Chung, J. Y.; Mason, J Polym Prepr 2007, 138, 1054828.
17. Hu, Y.; Schiraldi, D. A.; Hiltner, A.; Baer, E. Proceedings of 62nd Annual Technical Conference and Exhibition (Antec) 2004, May 16–20th, Chicago, Vol. 1 Processing, 1106.